Available online at www.sciencedirect.com
ScienceDirect
Journal of Power Sources 165 (2007) 244–252
JOURNAL OF POWER SOURCES
www.elsevier.com/locate/jpowsour

Exergoeconomic analysis of a vehicular PEM fuel cell system

S.O. Mert [a,b], I. Dincer [a,*], Z. Ozcelik [b]

[a] *Faculty of Engineering and Applied Sciences, University of Ontario Institute of Technology, Oshawa, Ontario, Canada*
[b] *Department of Chemical Engineering, Ege University, Izmir, Turkey*

Received 17 June 2006; received in revised form 28 November 2006; accepted 1 December 2006
Available online 16 January 2007

Abstract

In this study, we deal with the exergoeconomic analysis of a proton exchange membrane (PEM) fuel cell power system for transportation applications. The PEM fuel cell performance model, that is the polarization curve, is previously developed by one of the authors by using the some derived and developed equations in literature. The exergoeconomic analysis includes the PEM fuel cell stack and system components as compressor, humidifiers, pressure regulator and the cooling system. A parametric study is also conducted to investigate the system performance and cost behaviour of the components, depending on the operating temperature, operating pressure, membrane thickness, anode stoichiometry and cathode stoichiometry. For the system performance, energy and exergy efficiencies and power output are investigated in detail. It is found that with an increase of temperature and pressure and a decrease of membrane thickness the system efficiency increases which leads to a decrease in the overall production cost. The minimization of the production costs is very crucial in commercialization of the fuel cells in transportation sector.

Keywords: Energy; Exergy; Efficiency; PEM; Vehicle; Performance

1. Introduction

During the past decade, alternative fuels and power sources have received an increasing attention due to the increasing environmental pollution and the decrease of the fossil fuel resources. So a movement towards environmentally friendlier and more efficient power production sources both for stationary and mobile applications is of paramount importance and brings the fuel cells to the forefront.

Fuel cells are electrochemical devices that convert chemical energy of the reactants directly into electric and heat with high efficiency. Also, high operating temperature is not necessary for achieving high efficiency as the fossil fuels since electrochemical processes in fuel cells are not governed by Carnot's law. High efficiency makes fuel cells an attractive option for a wide range of applications, including transportation applications, domestic electricity, heat production and even portable and mobile systems.

PEM fuel cells are considered as the one of the most promising alternative power sources especially for sub-megawatt scale applications like light-duty transportation and considered as a potential replacement with the classical conventional internal combustion engines. A PEM fuel cell powered vehicle has a number of important advantages as high efficiency, quick start up, low operating temperatures, high current density and zero pollution. On the other hand, having high capital costs, problems of hydrogen storage and lack of infrastructure is the main problem for the commercialization of the PEM fuel cells in transportation applications. In these conditions, any increase in the system efficiency will help accelerate the commercialization of fuel celled vehicles [1].

Exergy analysis appears to be a potential for system design, analysis and process evaluation and improvement. Whereas energy analysis is based on the first law of thermodynamics, exergy analysis is based on both the first and the second laws of thermodynamics. Both analyses utilize also the material balance for the considered system. Analysis and optimization of any physical or chemical process, using the energy and exergy concepts, can provide the two different views of the considered process [2].

There are only few studies on the exergy analysis of PEM fuel cells for transportation applications. Hussain et al. [1] investi-

* Corresponding author. Tel.: +1 905 721 8668/2573; fax: +1 905 721 3370.
E-mail addresses: orcun.mert@ege.edu.tr, suhaorcun.mert@uoit.ca (S.O. Mert), ibrahim.dincer@uoit.ca (I. Dincer), zehra.ozcelik@ege.edu.tr (Z. Ozcelik).

0378-7753/$ – see front matter © 2006 Elsevier B.V. All rights reserved.
doi:10.1016/j.jpowsour.2006.12.002

Nomenclature

a	membrane activity
A_{cell}	cell area (cm^2)
AC_k	annual capital cost (US\$ $year^{-1}$)
C	exergetic cost (US\$ kW^{-1})
C_k	capital cost (US\$)
CRF(i, n)	capital recovery factor
e	exergy ($kW\,kg^{-1}$)
E	exergy, (kW)
F	Faradays constant (C)
$\dot{F}$	flow rate ($kmol\,s^{-1}$)
h	enthalpy ($J\,mole^{-1}$)
HHV	higher heating value ($kJ\,mole^{-1}$)
i	current density ($A\,cm^{-2}$); interest rate
i_o	exchange current density ($A\,cm^{-2}$)
I	irreversibility (kW)
n	life time, year
n_{cell}	number of fuel cells in stack
P	pressure (atm)
PW	present worth (US\$)
PWF(i, n)	present worth factor
R	resistance (Ω)
R	universal gas constant ($J\,(mole\,K)^{-1}$)
s	entropy ($J\,(K\,mole)^{-1}$)
$S_{k,n}$	salvage value (US\$)
t_{mem}	membrane thickness (cm)
T	temperature (K)
V	cell potential (V)
W	power (W)
x	mole fraction
Z	capital Cost flow (US\$ s^{-1})

Greek letters

α	transfer coefficients
η	efficiency
λ_{mem}	membrane water content
μ	chemical potential ($J\,mole^{-1}$)
σ_{mem}	membrane conductivity ($1\,(\Omega\,cm)^{-1}$)
ξ	stoichiometric ratio, ratio of excess air and fuel

Subscripts

A	anode
act	activation
C	cathode
ch	chemical
con	concentration
FC	fuel cell
irrev	irreversible
in	inlet
mem	membrane
ohm	ohmic
out	outlet
phy	physical
rev	reversible

gated thermodynamic analysis on fuel cell power systems. They studied the effects of operating temperature, operating pressure and air stoichiometry on the system performance. In addition to this study, Cownden et al. [3] performed exergy analysis of hydrogen fuel cell power system for bus transportation. Both of these two works showed the importance of the thermodynamic analysis in determining the irreversibilities within the system components and how the operating parameters affect the system performance. Ay et al. [4] derived a model for the thermodynamic analysis of a PEM fuel cell and found that thermodynamic irreversibilities in the fuel cell increase with a rise of membrane thickness and with a decrease of cell temperature and pressure. For a PEM fuel cell using methanol, an exergy analysis has been studied by Ishihara et al. [5]. It is found that the energy efficiency approaches the unity as the recovery rate of the waste heat from the cell approaches the unity. The exergy efficiency is found to be about 0.45 with a fuel cell operating temperature of 80 °C. It was also found that the cell voltage should exceed 0.82 V in order to obtain the exergy efficiency of 0.5 or higher. Moreover, Kazim [6] conducted exergy analysis of a PEM fuel cell at specified operating voltages of 0.5 and 0.6 V. In the study, the exergy efficiency of the PEM fuel cell is investigated depending on the operating temperature (T/T_0) and operating pressure (P/P_0) at the ratios ranging from 1 to 1.25 and from 1 to 3, respectively. Ay et al. [7] have proposed an exergetic performance analysis for a PEM fuel cell to investigate the effects of operating temperature and pressure to the system efficiency and irreversibilities. It is concluded in the paper that exergy efficiency of PEM fuel cell decreases with a rise in membrane thickness and current density, and increases with a rise of cell operating pressure and with a decrease of current density for the same membrane thickness. Kazim [8] also studied a brief exergoeconomic analysis of a PEM fuel cell at various operating temperatures, pressures and air stoichiometries. This study extends his previous study to cover the investigation of the air stoichiometry ranging from 2 to 4 from the exergy perspective. He indicated that the exergy cost of the fuel cell can be improved by adopting any or a combination of higher operating pressure, inlet air stoichiometry or cell voltage that demonstrates a significant improvement in the exergy cost. Barbir and Gomez [9] showed that there is a strong relationship between the efficiency and economics of PEM fuel cells. Typically, the lowest efficiency is achieved at maximum power output. The results indicate that in the best case scenario the fuel cells can be produced at US\$ 100 kW^{-1} with 50% efficiency, and generate electricity at cheaper than US\$ 0.08 kW^{-1} if hydrogen can be supplied at US\$ 10 GJ^{-1}.

Here, the present study differs from the above said studies since this investigates the effect of the operating parameters and some design parameters in a broad range including the system components other than the fuel cell stack, such as compressor, heat exchanger, humidifiers, pressure regulator and the cooling system on the system performance. Also, the present study investigates the exergetic cost flows of the system equipments and the total cost for the power production as an exergoeconomic analysis.

2. Exergoeconomic analysis

2.1. Exergetic aspects

Exergy analysis is an effective thermodynamic method of using the conservation of mass and conservation of energy principles together with the second law of thermodynamics for the design and analysis of thermal systems, and is an efficient technique for revealing whether or not and by how much it is possible to design more efficient power systems by reducing the inefficiencies [2].

The exergy concept was introduced to overcome limitations of the energy analysis. The exergy expresses the practical value of any substance (or any field matter, e.g., a heat radiation), and is defined as a maximum ability of this substance to perform work relative to human environment. Also, as Rosen and Dincer [2] pointed out, energy analysis embodied first law of thermodynamics only identifies external energy waste and losses, on the other hand, exergy takes entropy into account too by including irreversibilities. As a matter of fact, exergy is defined as the maximum theoretical work obtainable as the system interacts with its surroundings and comes to equilibrium. Once a system is in equilibrium with its surroundings, it is not possible to use the energy within the system to produce work. At this point, the exergy of the system has been completely destroyed. The state in which the system is in equilibrium with its surroundings is known as the dead state.

In order to calculate the exergy of a system, we must specify both the system and the surroundings. The reference environment is used to standardize the quantification of exergy. The reference environment or simply the environment is assumed to be a large, simple compressible system. The reference temperature is assumed to be uniform at T_0, and the pressure is assumed to be uniform at P_0. Also, it is assumed that the intensive properties of the environment are not significantly changed by any process. Therefore, the environment is modeled as a thermal reservoir at T_0. In the present study, the restricted reference environment is chosen as 298 K and 1 atm and the unrestricted reference state composed of the N_2, O_2, H_2O and CO_2 and Ar in the molar fractions 0.775, 0.206, 0.018, 0.0003 and 0.0007, respectively.

In general, there are several types of exergy as physical, kinetic, chemical, potential, nuclear, magnetic, electrical, etc. Here, we consider physical (E_{phy}), chemical (E_{ch}), kinetic (E_k) and potential (E_p) exergies only as

$$\dot{E} = \dot{E}_k + \dot{E}_p + \dot{E}_{phy} + \dot{E}_{ch} = \dot{m}(e_k + e_p + e_{phy} + e_{ch}) \quad (1)$$

The physical exergy is equal to the maximum amount of work obtainable when the stream of substance is brought from its initial state to the environmental state defined by P_0 and T_0 by physical process involving only thermal interaction with the environment.

$$e_{phy} = (h - h_0) - T_0(s - s_0) \quad (2)$$

where subscript 0 stands for the reference environment (restricted).

The chemical exergy is the exergy component associated with the departure of the chemical composition of a system from that of environment. The chemical exergy can be defined in a molar basis as:

$$e_{ch} = \sum_j x_j(\mu_{j,0} - \mu_{j,00}) \quad (3)$$

where x_j is the mole fraction of the species j in the flow; $\mu_{j,0}$ the chemical potential of species j in flow evaluated at T_0 and P_0; $\mu_{j,00}$ is the chemical potential of species j in the flow evaluated in the reference environment (unrestricted) [1].

2.2. Exergoeconomic aspects

Exergoeconomic analysis is a method combining both exergy analysis and cost accounting. The method provides a technique to evaluate the costs of inefficiencies and/or the costs of individual process streams, including intermediate and final products [10].

Exergoeconomics is nowadays a powerful tool to study and optimize a power system. The application field is the evaluation of utility costs as products or supplies of production plants, the energy costs between process operations or of an energy converter. Those costs are applicable in feasibility studies, in investment decisions, on comparing alternative techniques and operating conditions, in a cost-effective section of equipment during an installation, an exchange or expansion of an energy system [11].

The cost balance of a system may be written as [12]:

$$\sum(\dot{E}_{in,i}C_{in,i}) + \dot{Z}_{equipment} = \sum(\dot{E}_{out,i}C_{out,i}) + \dot{W}C_W \quad (4)$$

where $E_{in,i}$, $E_{out,i}$, $C_{in,i}$ and $C_{out,i}$ are the exergies and exergy costs of the streams entering and leaving the control volume, respectively. $\dot{Z}_{equipment}$ is the annualized cost of the equipment inside the control volume. C_W is the cost of the work or the power of the equipment. Using Eq. (4) the costs for the each component of the system is determined. Also, the cost balance is applied to the overall system to calculate the cost of the produced power by the fuel cell system.

In order to calculate $\dot{Z}_{equipment}$, the annualized (or levelized) cost method is used [13]. The algorithm of this method is composed of four steps as outlined by Kwak et al. [14]. The first the present worth (PW) of the investigated system is calculated by substituting the effect of salvage value, $S_{k,n}$ (Eq. (5)). In the calculations, the salvage values are taken as 10% of the capital cost.

$$PW_k = C_k - S_{k,n}PWF(i, n) \quad (5)$$

With the help of the CRF (capital recovery factor) that is, a function of the lifetime (n years) and interest rate (i), the annual capital cost is found, which is used for the calculation of the capital cost flow of the present system ($\dot{Z}_{equipment}$):

$$AC_k = PW \times CRF(i, n) \quad (6)$$

$$\dot{Z}_k = \frac{\phi_k AC_k}{3600\,s\,h^{-1} \times 8000\,h\,yr^{-1}} \quad (7)$$

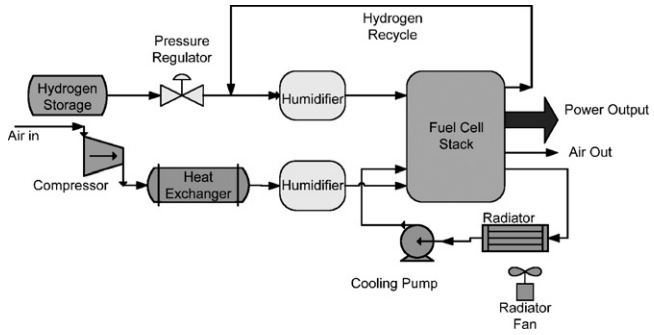

Fig. 1. Flow chart of Ballards Xcellsis™ HY-80 fuel cell engine [28].

$$\mathrm{CRF} = \frac{i(1+i)^n}{(1+i)^n - 1} \tag{8}$$

where PWF(i, n) is the present worth factor that is taken as 7.0236 [15], ϕ is the factor for the operating and maintenance costs which is taken as 1.06 of the AC. The lifetime of the system is taken as 10 years.

2.3. The fuel cell engine system studied

The Ballard's Xcellsis™ HY-80 Fuel Cell Engine is taken as an example system for model calculations (Fig. 1). This engine is used by many automobile producers like Ford in Focus Fuel Cell Vehicle (FCV) and MAN Fuel-cell bus [16]. The engine is lightweight, 68 kW hydrogen-fuelled fuel cell engine that offers automotive manufacturers the opportunity to develop their own zero-emission fuel cell vehicles. The Xcellsis™ HY-80 fits beneath the floor of the vehicle without reducing the size of the passenger compartment. It simplifies vehicle integration, assembly and service. The hydrogen stored in tank and fed to the system after a pressure regulation depending on the system pressure. Then, the inlet hydrogen is mixed with the recycled unreacted hydrogen from the fuel cell output. The final hydrogen stream is humidified in order to achieve the water management inside the stack. On the other hand, the air is introduced to the system via an air compressor. Air is pressurized up to the system operating pressure after that the temperature of air is adjusted to the operating temperature at the heat exchanger in which the outlet water stream from the fuel cell is used as coolant. The temperature of the fuel cell stack is maintained by a closed cooling system. Some of the total heat produced in the fuel cell stack is assumed to be lost by convection and radiation from the fuel cell stack. The remaining heat is taken by the cooling system and the outlet streams.

2.4. Modelling

2.4.1. Reversible cell voltage

The reversible cell voltage is the maximum voltage that the cell can be produce without any overpotentials and irreversibilities. There are numerous reversible cell voltage calculation equations developed in various forms of the Nernst equation. The equation developed by Amphlett et al. [17] is used since the equation depends on the data from the Ballard and is a function of environment temperature, system pressure and the partial pressures of both hydrogen and oxygen.

$$V_{\mathrm{rev}} = 1.229 - 8.5\times10^{-4}(T_{\mathrm{FC}} - 298.25) + 4.3085\times10^{-5} \times T_{\mathrm{FC}}\left[\ln(p_{\mathrm{H_2}}) + \tfrac{1}{2}\ln(p_{\mathrm{O_2}})\right] \tag{9}$$

The operating cell voltage is less then the reversible cell voltage because of the irreversibilities and overpotentials. The hydrogen and oxygen partial pressures may be calculated as:

$$p_{\mathrm{H_2}} = \frac{1 - x_{\mathrm{H_2O,A}}}{1 + (x_{\mathrm{A}}/2)(1+\xi_{\mathrm{A}}/(\xi_{\mathrm{A}}-1))} P_{\mathrm{A}} \tag{10}$$

$$p_{\mathrm{O_2}} = \frac{1 - x_{\mathrm{H_2O,C}}}{1 + (x_{\mathrm{C}}/2)(1+\xi_{\mathrm{C}}/(\xi_{\mathrm{C}}-1))} P_{\mathrm{C}} \tag{11}$$

where $x_{\mathrm{H_2O}}$ is the water mole fraction that is P_{sat}/P, respectively, both for anode and cathode. x_{A} and x_{C} are anode and cathode dry gas mole fractions, respectively, and ξ_{A} and ξ_{C} are anode and cathode stoichiometries, respectively [18].

2.4.2. Operating cell voltage

According to the reversible cell voltage, it is expected that the cell voltage remains constant during the operation of the fuel cell, but there are some overpotential losses that causes a voltage drop with respect to the current density. So the operating cell voltage may be expressed by:

$$V_{\mathrm{operating}} = V_{\mathrm{rev}} - V_{\mathrm{irrev}} \tag{12}$$

The overpotentials are mainly classified as: activation losses, ohmic losses, and concentration losses.

$$V_{\mathrm{irrev}} = V_{\mathrm{act}} + V_{\mathrm{ohm}} + V_{\mathrm{con}} \tag{13}$$

2.5. Activation overpotential

Activation losses are caused by low reaction rates in both anode and cathode by losing some of the energy while driving the reactions for transferring electrons. The relationship between the current density and overpotential is logarithmic. In this study, the activation losses are calculated by using the Tafel equations proposed by Barbir and Gomez [9] and Bard and Faulkner [19]. The overvoltage at the surface of an electrode follows a similar pattern in a great variety of electrochemical reactions [20]:

$$v_{\mathrm{act,Anode}} = \frac{RT_{\mathrm{FC}}}{\alpha_{\mathrm{A}} nF} \ln\left(\frac{i}{i_0}\right) \tag{14}$$

$$v_{\mathrm{act,Cathode}} = \frac{RT_{\mathrm{FC}}}{\alpha_{\mathrm{C}} nF} \ln\left(\frac{i}{i_0}\right) \tag{15}$$

where i is current density (A cm^{-2}); i_0 is exchange current density (A cm^{-2}); R is the universal gas constant (J (kmol K)$^{-1}$); n is the number electrons involved; F is the Faraday's constant (C mole^{-1}); α_{A} and α_{C} are the empirically determined electron transfer coefficient of the reaction at the electrodes at the anode and cathode. The exchange current density is higher if the reaction rate increases and can be considered as the current density at which the overvoltage begins to move from zero.

The i_0 exchange current density can be determined by empirical equation as derived by Berning [21]:

$$i_0(T) = 1.08 \times 10^{-21} \exp(0.086 \times T_{FC}) \quad (16)$$

2.5.1. Ohmic overpotential

Ohmic overpotential arises due to the electrical resistance inside the cell. The size of the voltage drop is proportional to the current. The resistance to the flow of protons in the membrane is much more effective than the resistance of the electrodes, resistance of the bipolar plates. The resistance to the flow of protons in the membrane is defined as the reciprocal of the proton conductivity in the membrane.

$$v_{ohm} = iR_{ohm} \quad (17)$$

$$R_{ohm} = \frac{t_{mem}}{\sigma_{mem}} \quad (18)$$

where σ_{mem} is the membrane conductivity ($1\,\Omega^{-1}\,cm^{-1}$).The membrane conductivity depends on the temperature and also on the water content of the membrane as:

$$\sigma_{mem} = (0.005139\lambda_{mem} - 0.00326) \exp\left[\frac{1268}{303} - \frac{1}{T_{FC}}\right] \quad (19)$$

where λ_{mem} is the membrane water content. The membrane water content is taken from Zawdonowski et al. [22]:

$$\lambda_{mem} = \begin{cases} 0.043 + 17.81a - 39.85a^2 + 39.85a^3, & 0 < a \le 1 \\ 14 + 1.4(a-1), & 1 < a \le 3 \end{cases} \quad (20)$$

$$a = \frac{x_{H_2O}P}{P_{sat}} \quad (21)$$

where a is the membrane water activity and x_{H_2O} is the water mole fraction.

2.5.2. Concentration overpotential

Because of the mass transfer limitations and the concentration drops at high current densities, some voltage drops occur in both anode and cathode. As the reaction proceeds, the concentration varies at the surface of the reaction sites and this will create a concentration gradient between the reaction sites and bulk phase. At high current densities, the concentration gradient will be very high and will limit the rate of reactions. Concentration overpotential is determined by the equation given by Guzzella [23].

$$v_{conc} = i\left(\beta_1 \frac{i}{i_{max}}\right)^{\beta_2} \quad (22)$$

where β_1 and β_2 and i_{max} are constants which depend on the operating temperature and reactant concentration. i_{max} and β_2 are taken as 2 also β_1 is calculated by the empirical equation of Pukrushkapan et al. [24]:

$$\beta_1 = \begin{cases} \text{If } \frac{p_{O_2}}{0.1173} + P_{sat} < 2, & (7.16 \times 10^{-4}T_{FC} - 0.622)\left(\frac{p_{O_2}}{0.1173} + P_{sat}\right) + (-1.45 \times 10^{-3}T_{FC} + 1.68) \\ \text{else}, & (8.66 \times 10^{-5}T_{FC} - 0.068)\left(\frac{p_{O_2}}{0.1173} + P_{sat}\right) + (-1.6 \times 10^{-4} + 0.54) \end{cases} \quad (23)$$

2.5.3. Fuel cell stack

Here, in this particular case, the fuel cell stack is composed of 97 cells of each having a 900 cm^2 effective area. The power produced by the stack can be calculated by:

$$\dot{W}_{Stack} = V_{operating} i A_{cell} n_{cell} \quad (24)$$

where n_{cell} is the number of fuel cells inside the stack; A_{cell} is the area of the each cell; i is the current density. The remaining exergy calculation for the fuel cell stack is done similar as the previous single fuel cell calculations.

2.5.4. Overall system

In order to determine the thermodynamic characteristics of the system, some general assumptions are made as follows:

- Both the PEM fuel cell and the fuel cell engine are assumed to be at steady state.
- The flows of reactants are incompressible and laminar.
- The gases are assumed as ideal.
- Hydrogen is stored at 10 bar and 298 K.
- Isentropic efficiencies are taken as 70% for compressor, cooling fan and cooling pump.
- 20% of the produced heat is assumed to be lost.
- The relative humidity of the inlet air and hydrogen is taken as 90%.
- The base operating parameters are 353 K temperature, 3 atm pressure, 0.016 cm membrane thickness, 1.5 for both anode and cathode stoichiometry.
- The cost for hydrogen is taken as US$ 10 GW [8].
- The capital costs of the system equipments are taken from Carlson et al. [25] as US$ 108 kW^{-1} for overall system

The overall exergy balance is:

$$\dot{I}_{FC} = \sum \dot{E}_{mass,in} - \sum \dot{E}_{mass,out} - \sum \dot{E}_{Heat} - \sum \dot{E}_{work}$$

In order to calculate the system efficiency, the net power production is calculated as:

$$\dot{W}_{net} = \dot{W}_{FC} - \dot{W}_{comp} - \dot{W}_{cool,pump,act} - \dot{W}_{fan,act} \quad (25)$$

$$\eta_{sys,energy} = \frac{\dot{W}_{net}}{HHV_{H_2}\dot{F}_{H_2,in}} \quad (26)$$

$$\eta_{sys,exergy} = \frac{\dot{W}_{net}}{\dot{E}_{in}} \quad (27)$$

where $\dot{E}_{in}$ is calculated from the exergies of the inlet streams of the system.

The overall exergetic cost balance can be written by using Eq. (4) as:

$$\sum(\dot{E}_{in,i}C_{in,i}) + \dot{Z}_{tot} = \sum(\dot{E}_{out,i}C_{out,i}) + \dot{W}_{net}C_W \quad (28)$$

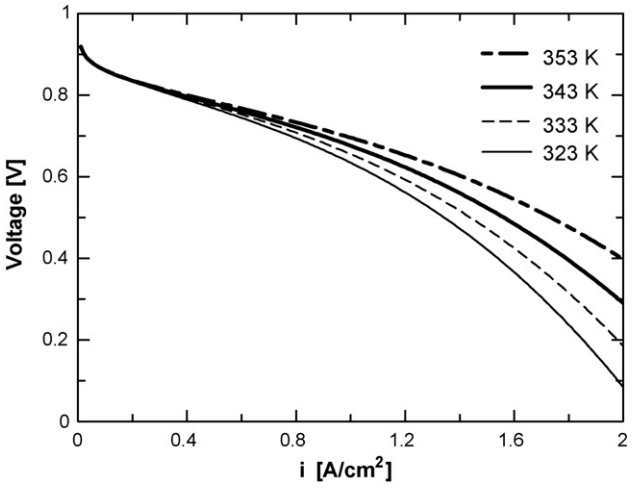

Fig. 2. Polarization curve for fuel cell engine system at different temperatures.

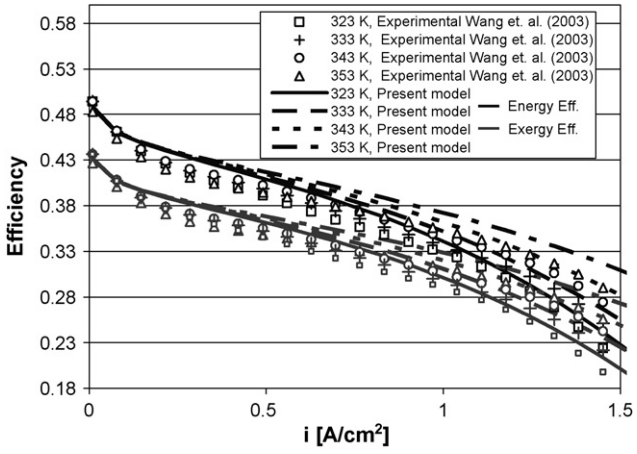

Fig. 3. Comparison of the present model with experimental data of Wang et al. [27].

3. Results and discussion

In order to investigate the fuel cell system performance, a parametric study is conducted. The operating parameters, such as temperature, pressure and stoichiometry ratio are considered for performance evaluation.

Fig. 2 shows how the polarization curve of the fuel cell changes with current density at various operating temperatures. The open-circuit voltage of the system lies between 0.85 and 0.9 V, primarily depending on the operating temperature. The operating parameters other than the investigated one for each study, in this case others than temperature, is kept constant in the best values, such as 3 atm pressure, 353 K temperature, 1.1 and 1.5 for fuel and air stoichiometry, respectively, and 0.016 cm membrane thickness. The effects of the overpotentials are clearly seen from this figure that the first region is the activation losses up to 0.25 A cm^{-2}, then the ohmic losses section up to 1.6 A cm^{-2}, finally the concentration and mass transport losses. It is also seen that the irreversibilities greatly depend on the current density as at the low current densities the cell voltage is nearly 0.9 V but at high values the voltage decreases up to 0.08 V. Fig. 2 also shows that with an increase of the operating temperature the cell voltage increases since the reversible cell voltage greatly depends on the operating temperature in a direct proportion and the overpotentials are less affected than the reversible cell voltage by operating temperature. The results of the present model are very consistent with some experimental studies in the literature [26,27]. Fig. 3 shows the comparison between the experimental results of Wang et al. [27] and the present model. It is seen that the trends of the efficiencies are very similar and the values matches greatly, more precisely there is a maximum error of 3% while the average error is about 1%. These small errors may arise from the use of empirical equations used and/or the effect of the deviations in operating parameters.

Fig. 4 shows that in low current densities, the efficiencies are increasing up to a peak point at 0.05 A cm^{-2} with 55% in energy efficiency and 48% in exergy efficiency. The reason for this is that the low current densities, the expenses as the compressor load, cooling pump load and the fan load are low when compared to the values at high current densities [1]. So after a critical point with an increase of the power withdrawn in the system the efficiencies start to decrease. When the current density reaches high values as 1.6 A cm^{-2} the energy efficiency values decreases in a rate higher than the exergy efficiency with results of nearly at 2 A cm^{-2} current density the efficiencies of the system decreased lesser than 5%. On the other hand, the effect of the temperature on the system efficiency can be seen from this graph. As similar to the polarization curve the efficiencies increases with increasing temperature and there is a difference of 8% for the high current densities means that the operating temperature is a crucial parameter for the fuel cells.

The main results for the study are the exergetic costs of the produced electricity from the engine including the expenses and all the system capital costs. As it is seen at low current densities, the low operating temperatures are cheaper than the high temperatures. But when the current densities higher than the 0.8 A cm^{-2}, the situation changes and the price of the electricity increases exponentially and the low temperatures becomes more expensive than high temperatures. This

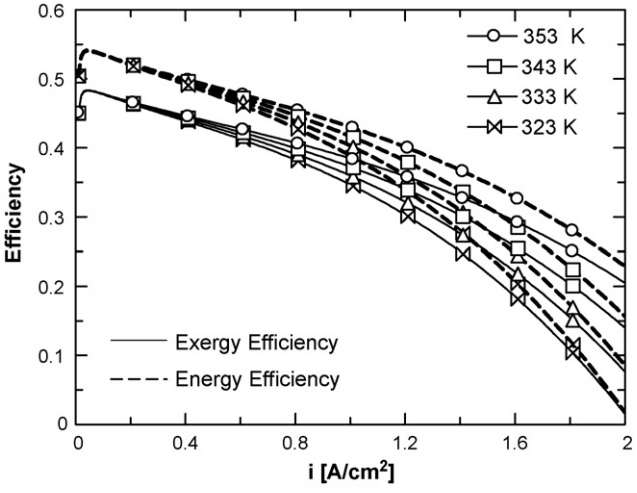

Fig. 4. Effect of temperature on the system performance.

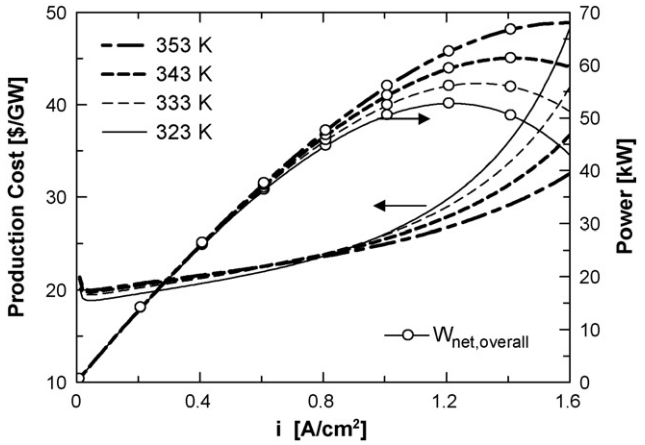

Fig. 5. The effect of the temperature on the overall costs and power produced.

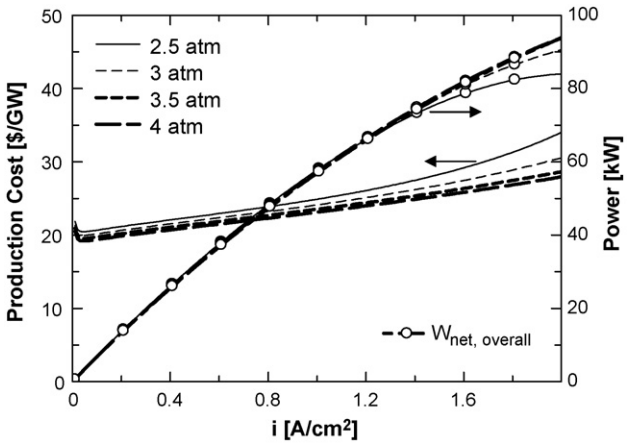

Fig. 7. Variations of production cost and network output with the current density at various operating pressures.

situation arises from the effects of the system components exergetic costs as the load of the heat exchanger changes for different temperatures and depending on the temperature the load of the humidifiers are also changes. Also, for the low operating temperatures in high current densities the costs are much higher because the produced electricity decreases as it is seen in the Fig. 5 and the efficiency decreases with the decreasing temperature as consistent with the study of Kazim [8].

The reversible cell voltage, ohmic overpotentials and concentration overpotentials are essentially pressure dependent, and these effects show a kind of nonlinear behaviour, so the effect of the pressure can only be investigated from these results. Increasing pressure increases the system efficiency as shown in Fig. 6. At high current densities the effect of pressure is more obvious with a difference of 5% in 1.8 A cm^{-2} current density but at low values gap between the 2.5 and 4 atm can be constant for up to 0.9 A cm^{-2} with an efficiency of 3%, respectively.

Although, high pressure operation requires pressurization of inlet streams that increases the compressor load, the net power production increases with the increasing pressure as it is seen from Fig. 7. Since the decrease in the overpotentials are higher than the increase in the compressor load that brings an increase in the overall efficiency with an increasing pressure. As it is expected, the effect of the pressure on the cost of the unit electricity production is in a positive way as shown in Fig. 7. Since the efficiency of the system increases depending on the pressure, the production cost for the 2.5 atm case is higher than the cost for the 4 atm case, there is a maximum of US$ 7 GW^{-1} difference between the two cases. The results for the effect of pressure are also consistent with experimental studies of Wang et al. [27].

The effect of the membrane thickness for the system performance is given in Fig. 8. It is seen that with increasing the membrane thickness the efficiency of the system decreases down to 2% for moderate current densities. As the thickness of the membrane increases, the network output also decreases as seen in Fig. 9. The effect is much clearer at the high current densities with a difference of 4 kW. This decrease is expected, since the ohmic overpotential losses highly depends on the membrane thickness. Of course, it must be considered that the fuel crossover effect which decreases the system efficiency at low membrane

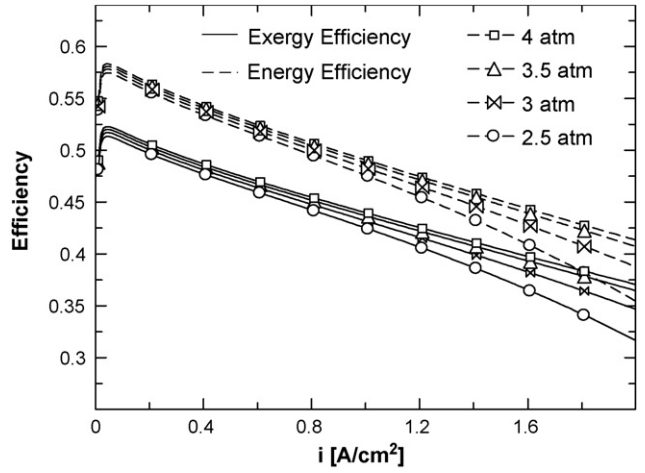

Fig. 6. Effect of pressure on the system performance in terms of energy and exergy efficiencies.

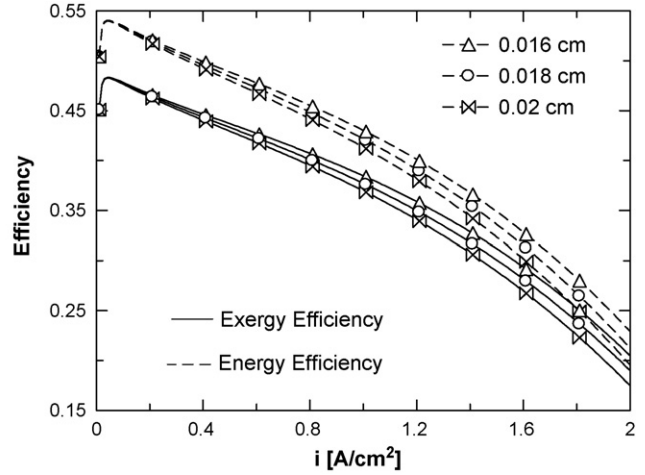

Fig. 8. Variation of energy and exergy efficiencies with the current density at various membrane thicknesses.

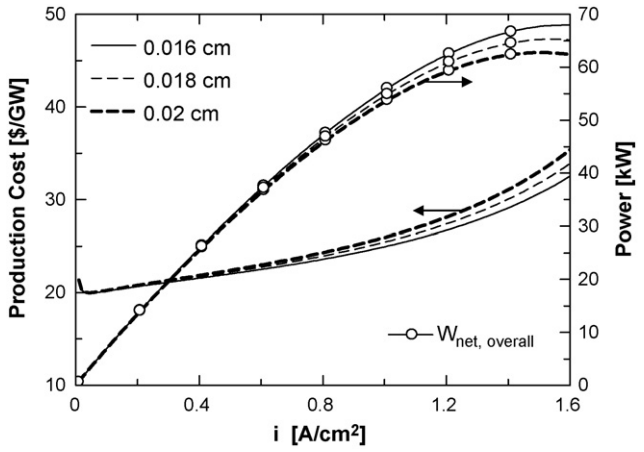

Fig. 9. Effect of membrane thickness on the production cost and power output.

thickness is neglected for this study and the fuel utilization ratios are kept constant depending on the fuel stoichiometry. Beside the efficiencies and power, the cost for electricity production is also affected directly by an increase of the membrane thickness (Fig. 9). The maximum difference appears to be US$ 3 GW^{-1} for the highest current density values at different thicknesses.

The effect of the cathode stoichiometry, which is the ratio of the fed oxygen to the required oxygen that gives the magnitude of the excess oxygen, on the system performance, is clearly shown in Fig. 10. By the increase of excess oxygen, the efficiency drops by about 1% since the exergy inlet to the system by the oxygen fed is increases but this increase does not causes a performance increment for the system so the efficiency of the system decreases dramatically. Fig. 11 shows the effect of the anode stoichiometry that means the ratio of the fed hydrogen to the required hydrogen to the system. Since the hydrogen is the main energy (fuel) source of the fuel cell, as expected the effect of the anode stoichiometry is very high on the efficiency values. With an increase of anode stoichiometry values from 1.1 to 3, the efficiency drops down to 35% with increasing current density.

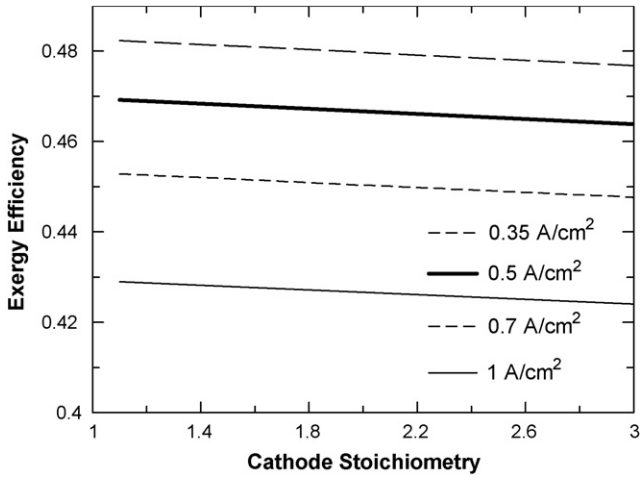

Fig. 10. Effect of cathode stoichiometry on exergy efficiency.

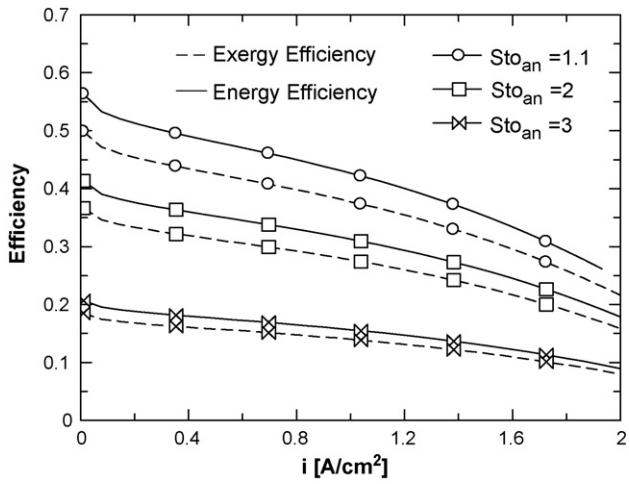

Fig. 11. Effect of anode stoichiometry on system performance in terms of energy and exergy efficiencies.

Fig. 12 shows the exergetic cost flows of the system equipment versus the current density. It is seen that the cost flows of the equipment do not depend on the current density. When these results are compared to the ones in Fig. 13, as the cost flows of the fuel cell stack in different temperatures with respect to the current density, it is seen that the cost of stack is much higher than costs for other components. These results are in agreement with the experimental data obtained by Carlson et al. [25]. Such a large difference means that the fuel cell stack is the most costly component based on the overall electricity production cost with having more than 40% contribution besides the stack cost is highly dependent to the current density since the maximum irreversibilities occur in fuel cell stack and these irreversibilities are highly dependent to the current density as activation and ohmic overpotentials. Also, the effect of the temperature to the fuel cell stack cost can be seen from Fig. 13, which is also compatible with the overall system cost since increasing temperature decreases the fuel cell stack cost.

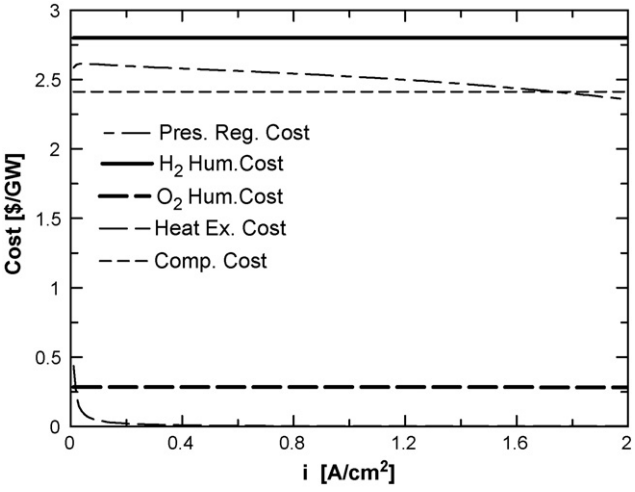

Fig. 12. System components cost vs. current density.

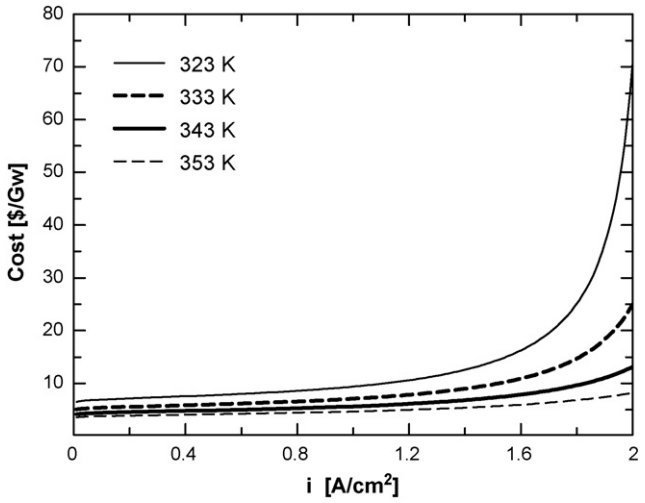

Fig. 13. Fuel cell stack cost vs. current density.

4. Conclusions

An exergoeconomic model has been developed and applied to a PEM fuel cell engine system for transportation applications. A parametric study is conducted to investigate the system performance and the cost behaviour depending on the operating parameters. It is found that, with an increase of operating temperature the system efficiency increases and the overall production costs decrease. Also, high pressure is another positive parameter for the system efficiency if we neglect the increase of manufacturing costs at higher pressures. The increase in the cathode stoichiometry leads to a small decrease in the overall system exergy efficiency, but the anode stoichiometry has a major effect on the efficiency. The main contribution to the overall cost is made by the fuel cell stack that has the highest irreversibility compared to the other system components. So any increase in the stack efficiency will greatly affect the overall performance and the production cost, and will contribute the commercialization of the fuel cell systems in the transportation sector.

Acknowledgement

The authors gratefully acknowledge the financial support provided by the Ontario Premier's Research Excellence Award, the Natural Sciences and Engineering Research Council of Canada and University of Ontario Institute of Technology in Canada and Ege University in Turkey.

References

[1] M.M. Hussain, J.J. Baschuk, X. Li, I. Dincer, Int. J. Therm. Sci. 44 (2005) 903–911.
[2] M. Rosen, I. Dincer, Energy Convers. Manage. 44 (2003) 1633–1651.
[3] R. Cownden, M. Nahon, M. Rosen, Exergy Int. J. 1 (2001) 112–121.
[4] M. Ay, A. Midilli, I. Dincer, Int. J. Exergy 3 (1) (2006) 16–44.
[5] A. Ishihara, S. Mitsushima, N. Kamiyab, K. Ota, J. Power Sources 126 (2004) 34–40.
[6] A. Kazim, Energy Convers. Manage. 45 (2004) 1949–1961.
[7] M. Ay, A. Midilli, I. Dincer, Int. J. Energy Res. 30 (2006) 307–332.
[8] A. Kazim, Energy Convers. Manage. 46 (2005) 1073–1081.
[9] F. Barbir, T. Gomez, Int. J. Hydrogen Energy 22 (10/11) (1997) 121–196.
[10] H. Chang, J. Sci. Eng. 4 (2) (2001) 94–104.
[11] J.L. Silveiraa, C.E. Tuna, Prog. Energy Combust. Sci. 29 (2003) 479–485.
[12] A. Bejan, G. Tsatsaronis, M. Moran, Thermal Design and Optimization, Wiley, New York, 1996.
[13] J. Moran, Availability Analysis: A Guide To Efficient Energy Use, Prentice-Hill Inc., Englewood Cliffs, 1982.
[14] H.-Y. Kwak, D.-J. Kim, J.-S. Jeon, Energy 28 (2003) 343–360.
[15] Michigan Department Of Environmental Quality Remediation And Redevelopment Division Financial Assurance Mechanisms (DOE), 2003, Present Worth analysis, Guidance document.
[16] Fuel Cells for Mobility, 2005, Fuel Cell Council, www.usfcc.com.
[17] J.C. Amphlett, R.M. Baumert, R.F. Mann, B.A. Peppley, P.R. Roberge, J. Electrochem. Soc. 142 (1) (1995) 9–15.
[18] A. Rowe, X. Li, J. Power Sources 102 (2001) 82–96.
[19] A.J. Bard, L.R. Faulkner, Electrochemical Methods, Wiley, New York, 1980.
[20] J. Larminie, A. Dicks, Fuel Cell Systems Explained, Wiley, New York, 2003.
[21] T. Berning, Three dimensional computational analysis of transport phenomena in a PEM fuel cell, Ph.D. Thesis, University of Victoria, Canada, 2002.
[22] T.A. Zawdonowski, T.E. Springer, S. Gottesfeld, J. Electrochem. Soc. 138 (8) (1991) 2334–2342.
[23] Guzzella, L., Control Oriented Modelling of Fuel-Cell Based Vehicle, Workshop on the Integration of Modelling And Control For Automotive Systems, NSF, 1999.
[24] J.T. Pukrushkapan, A.G. Stefenopoulou, H. Peng, Modelling and Control for PEM Fuel Cell Stack System, American Control Conference, Alaska, USA, 2002, TP09-2.
[25] E. Carlson, P. Kopf, J. Sinha, S. Sriramulu, Y.S Yang, PEM Fuel Cell Cost Status—2005 Fuel Cell Seminar, Cambridge, MA, November 14–18, 2005.
[26] F. Laurencelle, R. Chahine, J. Hamelin, K. Agbossou, M. Fournier, T.K. Bose, A. Laperriere, Fuel Cells 1 (1) (2001).
[27] L. Wang, A. Husar, T. Zhou, H. Liu, Int. J. Hydrogen Energy 28 (2003) 1263–1272.
[28] Ballard, 2005, Product Bulletin, Xcellsis™ HY-80 Fuel Cell Engine, www.ballard.com.